International Journal of Orthopaedics

Online Submissions: http://www.ghrnet.org/index.php/ijo
doi:10.17554/j.issn.2311-5106.2015.02.94

Int. J. Orthop. 2015 December 23 2(6): 468-475
ISSN 2311-5106.

ORIGINAL ARTICLE

A mouse femoral defect model demonstrates the clinically relevant side effects of BMP-2

Jia Shen, Omar Velasco, Kevork Khadarian, Greg Asatrian, Alan Hwang, Yulong Zhang, Jinny Kwak, Chirag Chawan, Kambiz Khalilinejad, Mark Ajalat, Tyler Pritchard, Xinli Zhang, Aaron W James, Chia Soo

Jia Shen, Omar Velasco, Greg Asatrian, Yulong Zhang, Jinny Kwak, Chirag Chawan, Kambiz Khalilinejad, Xinli Zhang, Aaron W James, Division of Growth and Development and Section of Orthodontics, School of Dentistry, University of California, Los Angeles, Los Angeles, CA9009, USA

Omar Velasco, Kevork Khadarian, Alan Hwang, Mark Ajalat, Tyler Pritchard, Aaron W James, Chia Soo, Department of Orthopaedic Surgery, University of California, Los Angeles, Los Angeles, CA 90095, USA

Omar Velasco, Department of Surgery, University of Maryland Medical Center, Baltimore, MD 21201, USA

Greg Asatrian, Aaron W James, Department of Pathology and Laboratory Medicine, University of California, Los Angeles, Los Angeles, CA 90095, USA

Yulong Zhang, Department of Bioengineering, Department of Materials Science and Engineering, and Division of Advanced Prosthodontics, University of California, Los Angeles, Los Angeles, CA 90095, USA

Chia Soo, Division of Plastic and Reconstructive Surgery, Department of Surgery, David Geffen School of Medicine, University of California, Los Angeles, Los Angeles, CA 90095, USA

Correspondence to: Chia Soo MD, Orthopaedic Hospital Department of Orthopaedic Surgery and the Orthopaedic Hospital Research Center; Division of Plastic and Reconstructive Surgery, Department of Surgery; MRL 2641A, 675 Charles E Young Dr. South, University of California, Los Angeles, Los Angeles, CA 90095-1579, USA.

Aaron W James MD, Department of Pathology and Laboratory Medicine; CHS A3-251, 10833 Le Conte Ave., University of California, Los Angeles, Los Angeles, CA 90095-1579, USA.

Email: awjames@mednet.ucla.edu/ bsoo@ucla.edu

Telephone: +91-33-22551275 Fax: +91-33-22879966

Received: July 11, 2015 Revised: September 25, 2015

Accepted: September 30, 2015

Published online: December 23, 2015

ABSTRACT

AIM: Bone morphogenetic protein-2 (BMP-2) is an FDA approved, osteoinductive growth factor for bone regeneration. However, increasing awareness of the side effects of BMP-2, including inflammation, bone resorption and fat formation, require the development of animal surgical models that replicate these adverse events.

MATERIAL AND METHODS: We devised a mouse femoral uni-cortical defect (UCD) model to study the clinical side effects of BMP-2. UCDs (3×1×1 mm) were drilled in one femur of mice and filled with poly(D,L-lactide-co-glycolide) (PLGA) scaffolding coated with PBS or rhBMP-2 (0.3mg/ml or 0.6mg/ml). Post mortem analyses were performed at four weeks post-surgery.

RESULTS: 100% successful surgery was achieved in mouse femoral UCD without surgical complication. Micro-CT analyses of the high dose rhBMP-2 group revealed bone cyst formation with ~2.5 fold increase in bone volume and more than 50% decrease in bone mineral density and trabecular number compared to PBS control. Tartrate-resistant acid phosphatase (TRAP) staining revealed a significant increase in osteoclast number, while immunostaining for fatty acid binding protein 4 (FABP4) and peroxisome proliferator-activated receptor gamma (PPAR-γ) confirmed significant increases in adipocyte formation with rhBMP-2 in a dose dependent manner. Lastly, rhBMP-2 treatment caused significant increases in inflammation, as determined by immunostaining for tumor necrosis factor-α (TNF- α) and interleukin 6 (IL6).

CONCLUSION: Here, we established a mouse UCD model that faithfully replicates the clinically reported side effects of rhBMP-2. This model may facilitate future studies to improve upon current efforts in rhBMP-2 based bone repair.

Key words: Bone Healing; Mice Model; Femoral Bone Defect; Bone Regeneration; Bone Morphogenetic Protein-2

Shen J, Velasco O, Khadarian K, Asatrian G, Hwang A, Zhang Y, Kwak J, Chawan C, Khalilinejad K, Ajalat M, Pritchard T, Zhang X, James AW, Soo C. A Mouse Femoral Defect Model Demonstrates the Clinically Relevant Side Effects of BMP-2. *International Journal of Orthopaedics* 2015; 2(6): 468-475 Available from: URL: http://www.ghrnet.org/index.php/IJO/article/view/1199

INTRODUCTION

Large bone defects in humans pose a treatment challenge to physicians, as these injuries often lead to clinical problems such as nonunion of the bones. In fact, approximately 10% of all fractures have incomplete or impaired healing[1]. Currently, bone grafts from autologous sites are the "gold standard"[2, 3, 4]. For many years, clinical scientists have been using various bone defects to investigate bone healing in small animal models[2]. In this study, we propose a small animal, uni-cortical defect (UCD) model that is able to recapitulate the clinically relevant side-effect profile of high doses of rhBMP-2. The UCD model is an easier, cost-effective and more replicable surgical procedure.

Scientists have used rodent femoral defect models to identify different growth factors and biomarkers, and to determine their efficacy in promoting bone regeneration. These growth factors include: BMP-2, Vascular Endothelial Growth Factor (VEGF), Nel-like Protein-1 (NELL-1), Platelet Rich Plasma (PRP), Erythropoietin (EPO) and stromal cell-derived factor 1 alpha (SDF-1a), to name a few[5, 6, 7]. Among all of these substances, BMP-2 has by far been the most extensively studied. The use of BMP-2 for bone healing has been granted FDA approval in limited clinical forms[8]. However, unregulated release of supraphysiologic amounts of BMP-2 has been shown to cause severe clinical side effects such as inflammation, ectopic bone formation, and osteoclast activation[9]. Inflammatory sequelae can be either mild (i.e. seroma formation or neuritis) or life threatening (i.e. cervical spinal swelling). This has led scientists to experiment with various methods of BMP-2 delivery, including demineralized bone matrices, collagen sponges, extracorporeal shock-waves, gene transfer, and different types of polymer scaffolds[10, 11, 12, 13, 14]. One of the primary concerns in deciding which delivery system to use is stress shielding in animal models. Bone plates and external fixation do not allow the appropriate amount of stress to transfer to the growing bone, which leads to its failure. Thus, the optimal scaffold for this usage is one that is biocompatible, biodegradable, and stiff enough to tolerate loads typically required from a femur[14]. The currently available and acceptable external[29] and internal mouse FSD model[30], the smaller dimensions of the high density material, rigid, moisture resistant, temperature durable, biocompatible plate and screws make these novel fixation systems costly. Development of a novel model that replicates the side effects of rhBMP-2 will significantly facilitate efforts in bone tissue engineering research.

METHODS

Animals and Surgical procedure

All animal experimentation was compliant with the UCLA Chancellor's Animal Research Committee. Eleven male CD1 mice were selected at 12 to 15 weeks of age. The groups consisted of the following: 0.01 M phosphate-buffered saline (PBS) + PLGA (*N*=4), 0.3mg/ml rhBMP-2 + PLGA (*N*=3), 0.6mg/ml rhBMP-2 + PLGA (*N*=4). The mice were given standard diet ad libitum during the preoperative and postoperative period. All CD1 mice (*N*=11) were anesthetized by isoflurane inhalation with a standardized weight-based dose. The right lower extremity was shaved with an electric shaver before prepping the surgical site with povidone-iodine topical antiseptic. An anterolateral longitudinal 10mm incision of the right thigh was performed. Cutaneous tissue was dissected and retracted to establish adequate exposure of the quadricep muscles. Vastus lateralis and quatratus femoris were identified and separated to gain access to the entire length of the femoral shaft. Using a drill mounted with a 0.5mm round fluted bur, two separate osteotomies 2mm apart were performed. Next, using the round fluted bur, the two osteotomies were connected to create a UCD. During the drilling process, beware not to inadvertently injure the endosteum of the opposing cortex, as this will deter an osteogenic response. Moreover, a metric ruler and standard field surgical telescopes (2.5×) were used to fine-tune the defect to the desired size of 3mm × 1mm × 1mm. The scaffolds were inserted into the defect site. The vastus lateralis and quatratus femoris was reapproximated over the defect site for soft tissue coverage. Finally, the skin was closed with 5-0 vicryl suture in a running continuous fashion. Postoperatively, analgesia was achieved with buprenorphine subcutaneous every 12 h for 48 h. TMP/SMX was given for 10 days for prevention of infection.

Preparation of Implants

Each implant was constructed as previously described[15]. The implants were coated with PBS, rhBMP-2 solution of 0.3mg/ml, or rhBMP-2 solution of 0.6mg/ml. The dimensions of the scaffolds were 3mm × 1mm × 1 mm. The volume of rhBMP-2 or PBS solution loaded on the respective scaffolds was 9.375ul.

Three-dimensional micro-computed tomographic evaluation

Once the mice reached 4 weeks postoperatively, the mice were euthanized using a carbon dioxide chamber. The femur that underwent the UCD procedure was dissected and harvested. Each femur was fixed in 4% paraformaldehyde for 48h, and analyzed using micro-CT scanner (Skyscan 1172F, Skyscan, Kontich, Belgium) at a 20μm (55kV and 181 mA radiation source, 0.5mm aluminum filter) resolution. The femoral defect site bone volume was measured and analyzed using DataViewer Recon, CTAn, and CTVol software provided by the manufacturer. Constant volume of interest was analyzed by centering the region of interest (ROIs) over the femoral defect site. The analysis consisted of the following: bone mineral density (BMD), bone volume/tissue volume (BV/TV), trabecular thickness (Tb.Th), trabecular spacing (Tb.Sp), and trabecular number (Tb.N). Newly formed bone was determined by using a global threshold technique (threshold value range of 60-120). All of the structural and quantitative parameters followed the nomenclature described by the American Society for Bone and Mineral Research Nomenclature Committee[16].

Antibodies and Reagents

Human rhBMP-2 (INFUSE Bone Graft) was purchased from Medtronic. Primary antibodies used in this study were anti-PPARγ (sc-7273, Santa Cruz Biotechnology, Santa Cruz, CA), anti-FABP4 (AF1443, R&D Systems, Minneapolis, MN), anti-TNFα (AF-510-NA, R&D Systems, Minneapolis, MN) and anti-IL6 (AF506, R&D Systems, Minneapolis, MN). All other reagents were purchased from Dako unless otherwise specified.

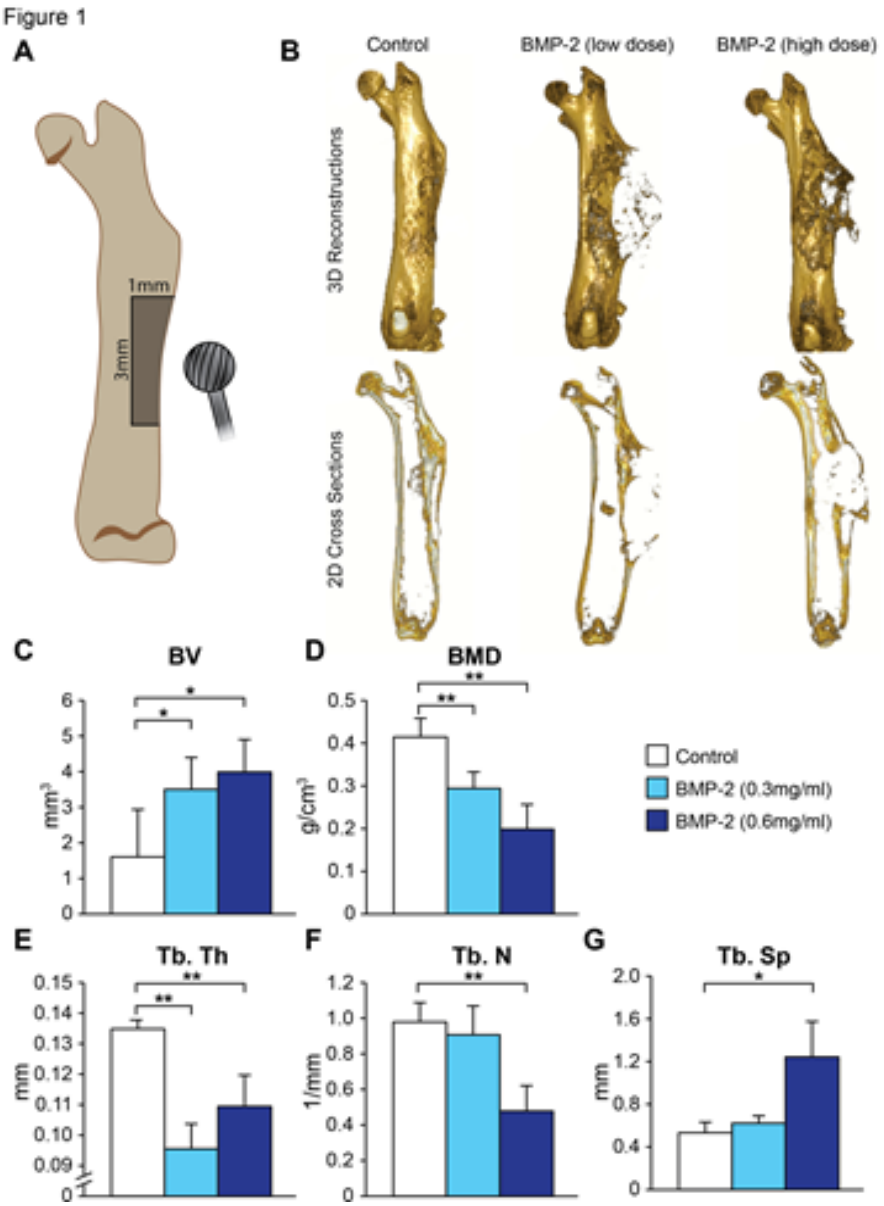

Figure 1 Bone healing after implantation of scaffolding. (A-E) MicroCT quantification of newly formed bone in and around the defect site, using the parameters of Bone Volume (BV), Bone Mineral Density (BMD), Trabecular Thickness (Tb.Th), Trabecular Number (Tb. N), and Trabecular Spacing (Tb.Sp). (F) Representative 3D reconstructions and 2D microCT images of femoral coronal sections from PBS and rhBMP-2 treatment groups; obtained using OsiriX imaging software. *p < 0.05; **p <0.01 compared to PBS control.

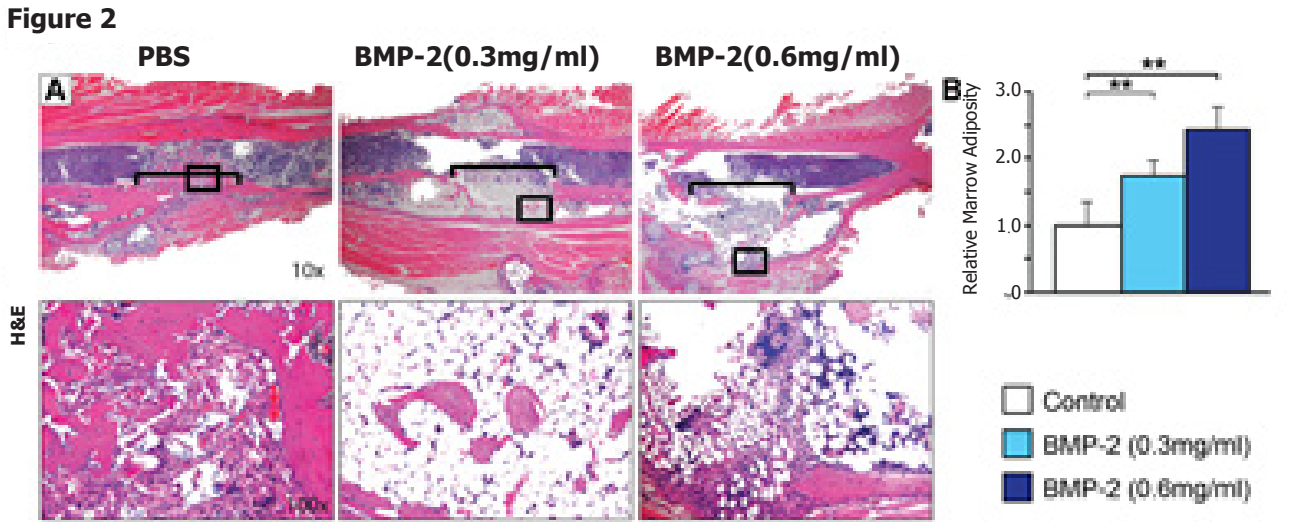

Figure 2 Histologic appearance and quantification after implantation of scaffolding. (A) H&E stained sections of the UCD site at low magnification (1000mm, top row) and high magnification (100mm, bottom row) demonstrate dramatic histologic changes after rhBMP-2 treatment. Brackets indicate defect site. High magnification images are of the region indicated by the rectangle in the corresponding low magnification image. (B) Quantification of marrow adiposity among PBS control or rhBMP-2 treatment groups. Quantification is expressed as the average relative marrow adiposity of six fields per sample, each taken at a 200 × magnification. Representative 10 × and 100 × images shown. **p < 0.01 compared to PBS control.

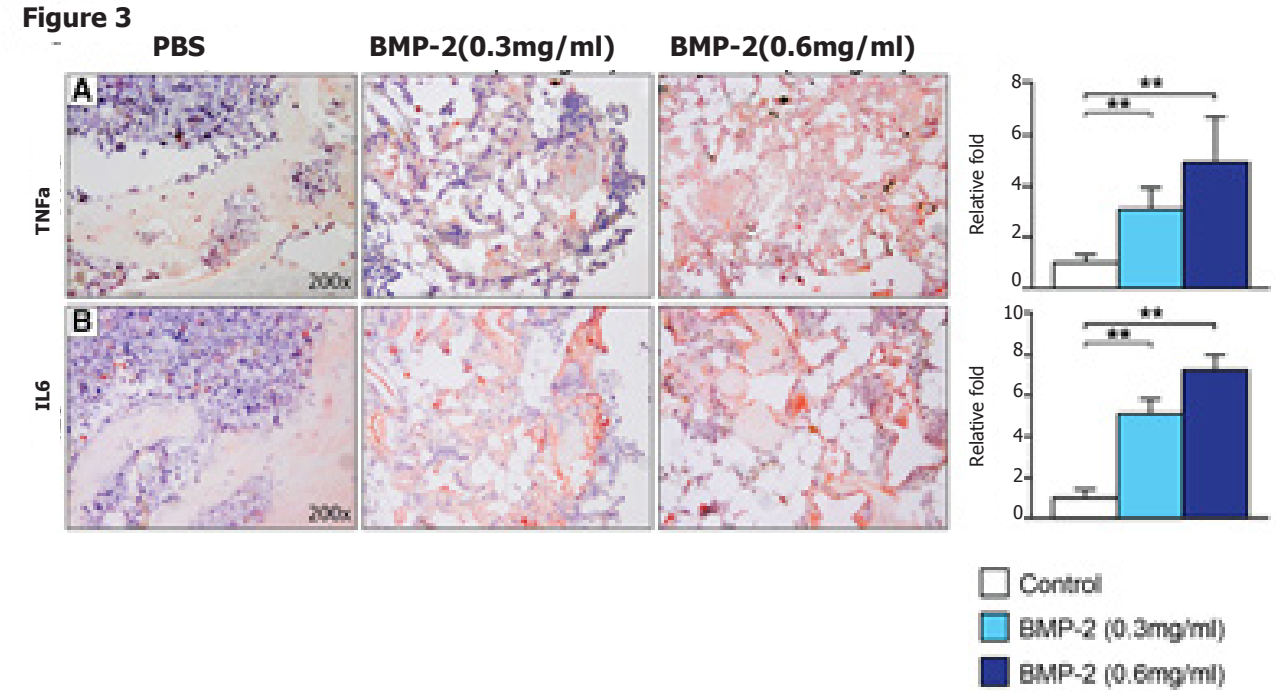

Figure 3: Immunohistochemical staining for markers of inflammation. Immunohistochemical staining and semi-quantification of TNFα(A) and IL6 (B) Semi-quantification is expressed as the average relative intensity of six fields around defect site per sample, each taken at a 200 × magnification. Semi-quantification is expressed as the average relative intensity of six fields per sample, each taken at a 200 × magnification. Representative images are shown at 200 ×. $^{**}p < 0.01$ compared to PBS control.

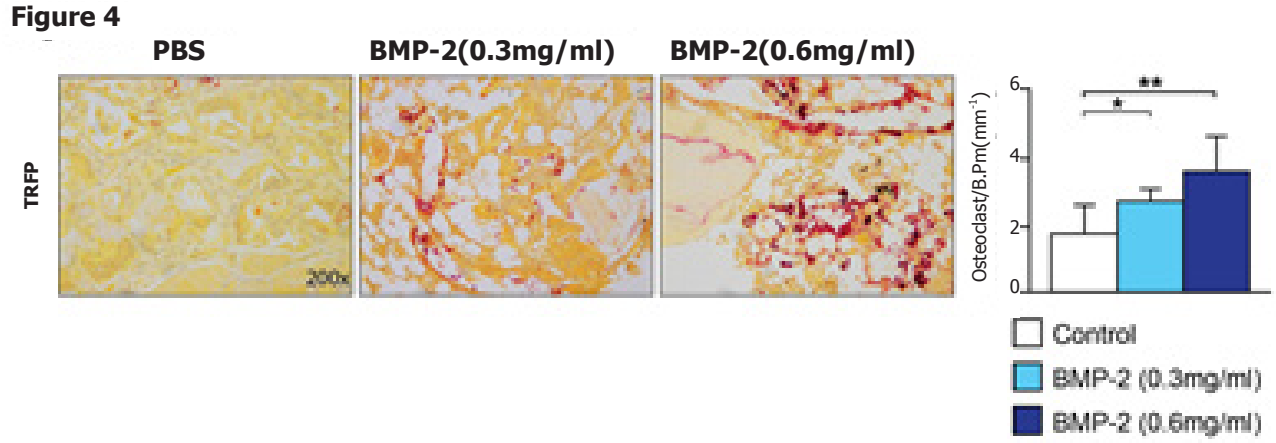

Figure 4: Detection of osteoclast markers after implantation of scaffolding. Histochemical staining and semi-quantification of Tartrate Resistant Acid Phosphatase (TRAP). Semi-quantification is expressed as the average number of TRAP+ osteoclasts per B.Pm. Six fields per sample, each taken at a magnification of 200 ×, were used for this quantification. Number of bone lining, TRAP+ osteoclasts was determined by two blinded observers. Representative images are shown at 200 ×. $^{*}p < 0.05$; $^{**}p < 0.01$ compared to PBS control.

Histology and Immunohistochemistry (IHC) analysis

Tissue from the femurs was decalcified using 19% Ethylenediaminetetraacetic acid (EDTA). Five-micron-thick paraffin sections of decalcified samples cut along the coronal plane were stained with H&E. Marrow adiposity of random 400x H&E sections (*N*=6 per group) were quantified using Adobe Photoshop, by comparing the area of adipose tissue to the area of the whole bone marrow. Additional sections were analyzed by indirect IHC. Briefly, unstained sections were deparaffinized and incubated with anti-TNFα, anti-IL6, anti-PPARγ, and anti-FABP4 primary antibodies and then by the appropriate biotinylated secondary antibodies (K1501, Dako, Carpinteria, CA). Positive immunoreactivity was detected following ABC complex (PK-6100, Vectastain Elite ABC Kit, Vector Laboratories Inc., Burlingame, CA) incubation and development with AEC chromagen (K346911-2, Dako, Carpinteria, CA). Photomicrographs were acquired using Olympus BX51 (400 x magnification lens, UPLanFL, Olympus). The relative intensity of TNFα, IL6, PPARγ, and FABP4 staining was analyzed using commercial software Image-Pro Plus 6 and quantified by the mean optical density of staining signal × per percent area positively stained × 100[17].

TRAP staining

TRAP staining was performed as previously described[18] and analyzed by three blinded observers and quantified by the number of osteoclasts per trabecular bone perimeter in millimeters. The observers analyzed and averaged the results from six random fields per sample.

Figure 5

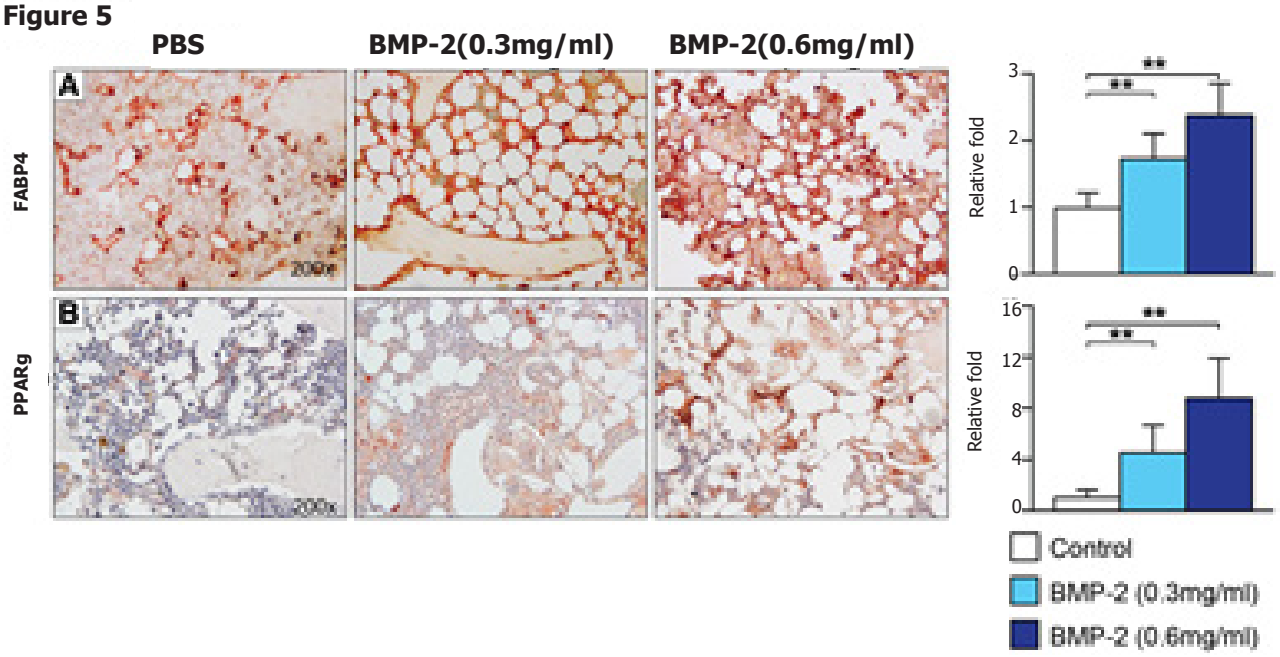

Figure 5: Adipogenic marker expression after implantation of scaffolding. Immunohistochemical staining and semi-quantification of FABP4 (A) and PPARγ (B). Semi-quantification is expressed as the average relative integrated intensity of staining around the defect site. Six fields per sample, each taken at a magnification of 200 ×, were used for this quantification. Representative images are shown at 200 ×. $^{**}p < 0.01$ compared to PBS control.

Statistical Analysis

To confirm our findings statistically, a one-way ANOVA (Analysis of Variance) was used to compare all three treatment groups. Subsequently, a post-hoc Tukey's test was performed to compare means between pairs of treatment groups. $^{*}P < 0.05$ and $^{**}P < 0.01$ were considered significant.

RESULTS

Characterization of modified UCD model in mice

To evaluate the relevant side effects of rhBMP-2 using a small animal model, a mouse long bone cortical defect was devised. We implemented the recently described uni-cortical rat model[19] to mice with modifications. Unlike the previously described UCD model, a PLGA scaffold implant was utilized instead of a HYA-PVA hydrogel. Small-sized defects (3mm × 1mm × 1mm) were created with minimal bleeding and no stress fractures based on 3D reconstruction micro-CT analysis (Figure 1A). All cortical defects were extended longitudinally to accommodate for implantation PLGA scaffold.

Our study evaluated the applicability of the UCD model in mice by comparing three different implant groups: PBS, 0.3mg/ml rhBMP-2, and 0.6mg/ml rhBMP-2. Upon gross examination, inspection of the PBS group revealed no cyst formation at the cortical defect site at 4 weeks. Bone-like tissue was evident at the cortical defect site. In rhBMP-2 treatment groups, a dose-dependent cyst formation was evident at 4 weeks. The higher rhBMP-2 group had a larger cyst formation.

Radiographic analysis

Immediately postharvest and fixation, femurs were scanned using high-resolution micro-CT to evaluate bone healing and quality in the defect site (Figure 1B). Consistent with previous findings[20], rhBMP-2 treatment resulted in a significant, dose-dependent increase in bone volume at the defect site (Figure 1C). However, there was an inverse correlation between the quality of bone formed at the defect sites and the concentration of rhBMP-2 implanted, as shown by BMD quantifications (Figure 1D). In particular, high dose (0.6mg/mL) rhBMP-2 treatment caused significant decreases in Tb.Th and Tb.N, characteristics suggestive of frail and poor quality bone[21] (Figure 1E,F). Moreover, a marked approximate 2.5 fold increase in Tb.Sp was observed in samples treated with high-dose rhBMP-2, indicating more porous orbicular architecture. Therefore, although rhBMP-2-treated samples exhibited more robust bone formation compared to PBS treatment, de novo bone exhibited cystic patterns of micro architecture.

Histological and Immunohistochemical analysis

Hematotoxylin & Eosin (H&E) Staining

Upon completion of radiographic analysis and decalcification, samples were sectioned and stained with H&E. Low magnification imaging revealed healthy bone healing in PBS-treated samples, sparse trabecular bone islands, and abundant adiposity and inflammation in rhBMP-2 treated samples (Figure 2A). High magnification imaging of H&E-stained samples revealed typical bone formation and healing with notable osteoid and corresponding bone-lining osteoblasts in PBS-treated samples. However, significant amounts of adipocytes and space between trabecular bone islands were observed in low-dose rhBMP-2-treated samples. Moreover, treatment with high-dose rhBMP-2 elicited a robust mononuclear inflammatory cell response, including lymphocytes and mast cells. Furthermore, significant interspersed adiposity was observed. Thus, quantifications for marrow adiposity were performed (Figure 2B), further confirming that both low and high dose rhBMP-2-treated samples possessed a more adipose-rich marrow (1.7 and 2.4 fold, respectively, compared to PBS-control).

Markers of inflammation

To investigate the inflammatory response post-surgery, IHC staining for TNFα and IL6 was performed. PBS-treated samples exhibited baseline levels of TNFα positive immunostaining as demonstrated

in previous defect models[22]. However, rhBMP-2 treatment elicited a significant and dose-dependent increase in TNFα-positive staining with approximately 3 and 5 fold increases in the low and high dose rhBMP-2 groups respectively, when compared to PBS control (Figure 3A). Next, immunostaining for IL6 was performed. Consistent with TNFα analyses, low and high dose rhBMP-2 treatment resulted in marked dose-dependent increases (approximately 5 and 7 fold, respectively) in IL6 staining when compared to PBS-treatment (Figure 3B). Thus, both low- (0.3mg/mL) and high- (0.6mg/mL) dose rhBMP-2 treatments elicit a significant and dose-dependent inflammatory response when implanted locally.

Marker of osteoclast activation

As rhBMP-2 has previously been shown to promote osteoclast activation and bone resorption[15], we sought to investigate osteoclast number in samples treated with rhBMP-2 via TRAP staining. Consistent with previously published literature[22], PBS-treated samples exhibited baseline levels of osteoclast expression, whereas rhBMP-2 treated samples displayed significant increases in osteoclast expression, in a dose-dependent manner. Quantifications revealed a 1.5 and 2.0 fold increases in TRAP positive cells in low and high-dose rhBMP-2 treatment groups respectively, when compared to PBS-treated samples (Figure 4).

Markers for adiposity

Next, immunostaining for the adipose markers, FABP4 and PPARγ was performed. PBS-treated samples exhibited minimal FABP4 staining interspersed in the marrow space between bony islands. Both low and high dose rhBMP-2 treatment exhibited significantly increased positive staining, both qualitatively and quantitatively with approximately 1.5 and 2.5 fold increases, respectively, when compared to PBS-treated controls (Figure 5A). More dramatic and significant increases of approximately 4 and 8 folds were observed when immunostaining for PPARγ was performed, similarly in a dose-dependent manner (Figure 5B). Thus, we confirmed that rhBMP-2 treatment promotes significant adipogenesis and cystic bone formation when

DISCUSSION

In the present study, the rhBMP-2 treatment appears to promote bone formation in a mouse femoral UCD model. A marked increase in bone volume was seen, but the quality of bone was severely compromised in both low- and high-dose rhBMP-2 treatment. This decrease in bone microarchitecture was confirmed by significant decreases in BMD and trabecular bone parameters. The rhBMP-2 treatment elicited an inflammatory response and adipogenesis with marked activation of bone-lining osteoclasts. Although there are many different fixation models, the proposed UCD model provides a possible blueprint for future experiments with femoral bone defects in rodents.

The many different internal fixation models contain a number of technical challenges. Stainless steel, titanium, and polymeric plates have been used for customizing the plate in order to minimize disturbance of the region of interest when removing the bone screws[31-33]. Because an internal plate contacts the bone, this allows researchers to use it as a support for scaffolds, fibrin gels, and other softer materials used to deliver growth factors and stem cells[27,34,33,35]. Drawbacks to internal fixation using plates include the high cost of the necessarily biocompatible plates[32]. In addition, it is technically more difficult to install than intramedullary fixation, which is another method of internal fixation[18]. Finally, the costs associated with this procedure are higher compared to both intramedullary and external fixation[36]. This successfully developed model will allow scientists a less costly and more convenient way to study the effects of rhBMP-2 in conjunction with other biomaterials, as is currently done in the field as another way to improve clinical use of rhBMP-2.

Additionally, using small animal models has allowed for a simpler means to study fracture bone healing. Researchers interested in studying bone healing require a reliable and stabile fracture model. The smaller dimensions of a mouse model require the bone-stabilizing construct to possess specific qualities, such as being lightweight, of high density material, rigid, moisture resistant, temperature durable, biocompatible, and cost effective. In the present study, the UCD model in mice contains the majority of the stability features listed above, along with the advantages of potential for bilateral evaluation in the same animal and low stress fracture complications. Its fixation independence and unperturbed uni-cortical layer account for the overall biomechanics of the UCD model. This supports the UCD model in mice as a reliable means for studying the clinically relevant side effect profile of rhBMP-2.

The minimal periosteal callus formation is related to mechanical stiffness of the UCD model in mice. Our PLGA-rhBMP-2 groups significantly accelerated the bone healing of the uni-cortical femoral defect. Specifically, the greater rhBMP-2 dose produced excessive bone formation with histological evidence of bone cyst and ectopic bone formation. The rhBMP-2 treatment groups had a significant, dose dependent increase in bone volume. This shows, once again, the bone-healing capabilities of rhBMP-2 as well as the clinical problems that are associated with it. In the UCD model, the defect is not critically sized, so the ideal treatment would be accelerated bone healing with no ectopic bone formation. Further studies that change the experimental conditions, conducted with the UCD mouse model, may yield a more ideal combination of protein factors, carrier material, and rhBMP-2.

The use of PLGA as a carrier for rhBMP-2 has long been described[12, 13]. It is a bioresorbable copolymer that can be prepared with rhBMP-2 and facilitates easy mixing and injection. The PLGA used in this experiment served as an effective carrier for rhBMP-2 in the mouse UCD model. The experiment manifested the expected side effects of excessive bone bridging, sparse trabecular bone islands, abundant adiposity and inflammation on histological evidence. Many other types of rhBMP-2 carriers have previously been used in the investigation of bone healing in rodents. However, some of the considerations in deciding which carrier to use can be circumvented with the UCD model. In critically sized defect studies, the stiffness of the scaffold is an important consideration, but with the UCD model, it is less important due to the smaller size of the defect[23]. One carrier consideration that remains important is its release profile of rhBMP-2[13]. The rhBMP-2 release profile has been shown to affect the amount of bone growth and future studies may find a more ideal carrier scaffold that prevents the side effects associated with rhBMP-2, which include postoperative soft tissue swelling, increased length of stay in the hospital, airway obstructions, tracheotomies, dyspnea, respiratory failure, ectopic bone growth, and perineural cysts[24]. The mouse UCD is likely to be applicable to other carrier scaffolds, therefore facilitating the investigation of the ideal method of delivering rhBMP-2. In recent studies, SDF-1a and Nell-1 have been used in conjunction with rhBMP-2 to avoid the unwanted effects of rhBMP-2.

In our study, the uni-cortical femoral defect eliminates the concern of inappropriate stress transfer by eliminating the need for any plate

or external fixation apparatus. This model reduces the cost and simplifies the procedure, circumventing the need to install an internal locking plate as is required with a femoral segmental defect model. Additionally, this model proves capable of assessing multiple side effects of BMP-2.

Abbreviations

ANOVA: Analysis of variance;
BMD: Bone Mineral Density;
BMP-2: Bone morphogenetic protein-2;
BV/TV: Bone Volume/Tissue volume;
EDTA: Ethylenediaminetetracetic acid;
EPO: Erythropoietin;
FABP4: Fatty acid binding protein 4;
FDA: Food and Drug Association;
H&E: Hematotoxylin & Eosin;
IL6: Interleukin 6;
NELL-1: Nel-like Protein-1;
PBS: Phosphate-buffered Saline;
PLGA: Poly(D,L-lactide-co-glycolide;
PPAR- γ: Peroxisome proliferator-activated receptor γ;
PRP: Platelet Rich Plasma;
ROI: Region of Interest;
Tb.N: Trabecular number;
Tb.Sp: Trabecular spacing;
Tb.Th: Trabecular thickness;
TGF: Tissue Growth Factor;
TNF- α: Tumor necrosis factor- α;
TRAP: Tartrate-resistant acid phosphatase;
UCD: Unicortical Defect;
VEGF: Vascular Endothelial Growth Factor.

ACKNOWLEDGMENTS

This work was supported by the CIRM Early Translational II Research Award TR2-01821, NIH/NIDCR (grants R21 DE0177711 and R01 DE01607), NIAMS (grant R01 AR061399-01A1), the Department of Pathology and Laboratory Medicine and the Translational Research Fund, UC Discovery Grant 07-10677, Eli & Edythe Broad Center of Regenerative Medicine and Stem Cell Research at UCLA Innovation Award.

REFERENCES

1. Logeart-Avramoglou D, Anagnostou F, Bizios R, Petite H. Engineering bone: challenges and obstacles. *Journal of cellular and molecular medicine* 2005; 9: 72-84
2. Reichert JC, Saifzadeh S, Wullschleger ME, Epari DR, Schutz MA, Duda GN, Schell H, van Griensven M, Redl H, Hutmacher DW. The challenge of establishing preclinical models for segmental bone defect research. *Biomaterials* 2009; 30: 2149-2163
3. Reichert JC, Cipitria A, Epari DR, Saifzadeh S, Krishnakanth P, Berner A, Woodruff MA, Schell H, Mehta M, Schuetz MA, Duda GN, Hutmacher DW. A tissue engineering solution for segmental defect regeneration in load-bearing long bones. *Science translational medicine* 2012; 4: 141ra193
4. Wheeler DL, Enneking WF. Allograft bone decreases in strength in vivo over time. *Clinical orthopaedics and related research* 2005; 36-42
5. Lee K, Silva EA, Mooney DJ. Growth factor delivery-based tissue engineering: general approaches and a review of recent developments. *Journal of the Royal Society, Interface / the Royal Society* 2011; 8: 153-170
6. Herberg S, Fulzele S, Yang N, Shi X, Hess M, Periyasamy-Thandavan S, Hamrick MW, Isales CM, Hill WD. Stromal cell-derived factor-1beta potentiates bone morphogenetic protein-2-stimulated osteoinduction of genetically engineered bone marrow-derived mesenchymal stem cells in vitro. *Tissue engineering Part A* 2013; 19: 1-13
7. Zhang X, Zara J, Siu RK, Ting K, Soo C. The role of NELL-1, a growth factor associated with craniosynostosis, in promoting bone regeneration. *Journal of dental research* 2010; 89: 865-878
8. Mont MA, Ragland PS, Biggins B, Friedlaender G, Patel T, Cook S, Etienne G, Shimmin A, Kildey R, Rueger DC, Einhorn TA. Use of bone morphogenetic proteins for musculoskeletal applications. An overview. *The Journal of bone and joint surgery American volume* 2004; 86-A Suppl 2: 41-55
9. Benglis D, Wang MY, Levi AD. A comprehensive review of the safety profile of bone morphogenetic protein in spine surgery. *Neurosurgery* 2008; 62: ONS423-431
10. Hsu WK, Sugiyama O, Park SH, Conduah A, Feeley BT, Liu NQ, Krenek L, Virk MS, An DS, Chen IS, Lieberman JR. Lentiviral-mediated BMP-2 gene transfer enhances healing of segmental femoral defects in rats. *Bone* 2007; 40: 931-938
11. Feighan JE, Davy D, Prewett AB, Stevenson S. Induction of bone by a demineralized bone matrix gel: a study in a rat femoral defect model. *Journal of orthopaedic research: official publication of the Orthopaedic Research Society* 1995; 13: 881-891
12. Lee SC, Shea M, Battle MA, Kozitza K, Ron E, Turek T, Schaub RG, Hayes WC. Healing of large segmental defects in rat femurs is aided by RhBMP-2 in PLGA matrix. *Journal of biomedical materials research* 1994; 28: 1149-1156
13. Brown KV, Li B, Guda T, Perrien DS, Guelcher SA, Wenke JC. Improving bone formation in a rat femur segmental defect by controlling bone morphogenetic protein-2 release. *Tissue engineering Part A* 2011; 17: 1735-1746
14. Chu TM, Warden SJ, Turner CH, Stewart RL. Segmental bone regeneration using a load-bearing biodegradable carrier of bone morphogenetic protein-2. *Biomaterials* 2007; 28: 459-467
15. Zara JN, Siu RK, Zhang X, Shen J, Ngo R, Lee M, Li W, Chiang M, Chung J, Kwak J, Wu BM, Ting K, Soo C. High doses of bone morphogenetic protein 2 induce structurally abnormal bone and inflammation in vivo. *Tissue engineering Part A* 2011; 17: 1389-1399
16. Parfitt AM, Drezner MK, Glorieux FH, Kanis JA, Malluche H, Meunier PJ, Ott SM, Recker RR. Bone histomorphometry: standardization of nomenclature, symbols, and units. Report of the ASBMR Histomorphometry Nomenclature Committee. *Journal of bone and mineral research: the official journal of the American Society for Bone and Mineral Research* 1987; 2: 595-610
17. Prasad K, P. BK, Chakravarthy M, Prabhu G. Applications of 'TissueQuant'- A color intensity quantification tool for medical research. *Comput Methods Prog Biomed* 2012; 106: 27-36
18. James AW, Shen J, Khadarian KA, Pang S, Chung G, Goyal R, Asatrian G, Velasco O, Kim J, Zhang X, Ting K, Soo C. Lentiviral delivery of PPARgamma shRNA Alters the Balance of Osteogenesis and Adipogenesis, Improving Bone Microarchitecture. *Tissue engineering Part A* 2014;
19. Hulsart-Billstrom G, Bergman K, Andersson B, Hilborn J, Larsson S, Jonsson KB. A uni-cortical femoral defect model in the rat: evaluation using injectable hyaluronan hydrogel as a carrier for bone morphogenetic protein-2. *Journal of tissue engineering and regenerative medicine* 2012;
20. Shintani N, Siebenrock KA, Hunziker EB. TGF-ss1 enhances the BMP-2-induced chondrogenesis of bovine synovial explants and arrests downstream differentiation at an early stage of hypertrophy. *PloS one* 2013; 8: e53086
21. Yu WS, Chan KY, Yu FW, Yeung HY, Ng BK, Lee KM, Lam TP, Cheng JC. Abnormal bone quality versus low bone mineral den-

sity in adolescent idiopathic scoliosis: a case-control study with in vivo high-resolution peripheral quantitative computed tomography. *The spine journal: official journal of the North American Spine Society* 2013; 13: 1493-1499

22. Elgali I, Igawa K, Palmquist A, Lenneras M, Xia W, Choi S, Chung UI, Omar O, Thomsen P. Molecular and structural patterns of bone regeneration in surgically created defects containing bone substitutes. *Biomaterials* 2014; 35: 3229-3242
23. Chen YJ, Wurtz T, Wang CJ, Kuo YR, Yang KD, Huang HC, Wang FS. Recruitment of mesenchymal stem cells and expression of TGF-beta 1 and VEGF in the early stage of shock wave-promoted bone regeneration of segmental defect in rats. *Journal of orthopaedic research: official publication of the Orthopaedic Research Society* 2004; 22: 526-534
24. Epstein NE. Pros, cons, and costs of INFUSE in spinal surgery. *Surgical neurology international* 2011; 2: 10